Author/s:
Kozorog, M;Sani, MA;Separovic, F;Anderluh, G

Title:
Listeriolysin O Binding Affects Cholesterol and Phospholipid Acyl Chain Dynamics in Fluid Cholesterol-Rich Bilayers

Date:
2018-09-20

Citation:
Kozorog, M., Sani, M. A., Separovic, F. & Anderluh, G. (2018). Listeriolysin O Binding Affects Cholesterol and Phospholipid Acyl Chain Dynamics in Fluid Cholesterol-Rich Bilayers. Chemistry A European Journal, 24 (53), pp.14220-14225. https://doi.org/10.1002/chem.201802575.

Author Manuscript

Title: Listeriolysin O binding affects cholesterol and phospholipid acyl chain dynamics in fluid cholesterol-rich bilayers

Authors: Mirijam Kozorog; Marc-Antoine Sani; Frances Separovic; Gregor Anderluh

To be cited as: 10.1002/chem.201802575

Link to VoR: https://doi.org/10.1002/chem.201802575

Listeriolysin O binding affects cholesterol and phospholipid acyl chain dynamics in fluid cholesterol-rich bilayers

Mirijam Kozorog,[a] Marc-Antoine Sani,[b] Frances Separovic,*[b] and Gregor Anderluh*[a]

Abstract: Listeriolysin O (LLO) is a pore-forming toxin that enables survival and cell-to-cell spread of food borne bacterial pathogen *Listeria monocytogenes*, responsible for the life-threatening disease, listeriosis. LLO-membrane interactions are crucial for pathogenicity of Listeria, but remained unexplained in detail at the molecular level. Here we addressed them by ^{2}H, ^{31}P, ^{13}C and ^{19}F solid-state NMR spectroscopy. Different fluid and ordered cholesterol-rich membrane lipid bilayer systems were prepared and checked for the integrity and properties in the presence of LLO. LLO has significantly changed dynamics of phospholipid acyl chains of more fluid cholesterol-rich bilayers, whereas the lipid bilayer organization was not affected. LLO has also affected cholesterol dynamics by increasing the intensity of low frequency motions, indicating direct interactions of LLO with cholesterol. Additionally, the LLO protein was shown to interact differently with lipid membranes, depending on the properties of cholesterol-rich membranes. The presented results, therefore, provide new insights into the interactions of the bacterial toxin LLO with cholesterol-rich membrane systems.

Introduction

Listeriolysin O (LLO) is the main virulence factor of the Gram-positive pathogenic bacterium *Listeria monocytogenes* that causes foodborne disease listeriosis [1]. The bacterium enters the host organism through the ingestion of contaminated food and is entrapped into the acidic phagolysosome. In order to survive, *L. monocytogenes* secrets LLO, a pore-forming toxin (PFT) which forms large membrane pores that enable bacterial escape from the phagolysosome, allowing its survival, cytosolic replication and subsequent cell-to-cell spreading [2]. LLO belongs to a family of cholesterol-dependent cytolysins (CDCs), a large group of PFTs, produced by various bacterial species [3]. CDCs share high sequence (40% – 70%) and structural similarity as seen from the determined tertiary structures, for example of LLO and perfringolysin O from bacterium *Clostridium perfringens* (PFO) [4], the most studied CDC representative. Amongst the CDCs, LLO possesses the unique feature of having highest stability and, subsequently, activity in acidic environments (pH 5.5). The activity is severely decreased in neutral pH at higher temperatures (above 30°C) due to protein aggregation [5], enabling protein inactivation when the bacteria enter the pH-neutral cytosol. Like all CDCs, LLO consists of 4 structural domains [4a], each having a distinctive role in the pore-forming process. The domain 4 is a β-sandwich fold containing three structural loops and a highly conserved tryptophan-rich undecapeptide at the base of the molecule. This region is responsible for membrane binding, which is followed by oligomerization of up to 50 monomeric molecules into a pre-pore assembly. Further, structural changes in Domain 2 cause the collapse of the molecule and its insertion into the membrane upon rearrangement of two clusters of α-helices within Domain 3 into amphiphilic β-hairpins that form the final β-barrel transmembrane pore [3a, b, 4a, 6].

For efficient binding, CDCs require high amounts of cholesterol in host membranes, exceeding 30% in exclusively phosphatidylcholine (PC) membrane systems as shown for LLO, and other CDCs such as PFO, streptolysin O and tetanolysin [7]. The double bonds in phospholipid acyl chains or the presence of phospholipids with smaller headgroups, however, reduce the cholesterol threshold that enables efficient binding of CDC molecules [8]. The same was achieved by the incorporation of longer acyl chain phospholipids or the partial replacement of PC with phosphatidylethanolamine (PE) [7c]. On the other hand, the addition of sphingomyelin (SM), a lipid associated with lipid domains or 'rafts', inhibited PFO association with the cholesterol-rich membranes [8a]. It was proposed that the accessibility of cholesterol at the membrane surface plays a critical role in CDC binding, being dependent on cholesterol solubility in the lipid membrane and only available for binding after the saturation point is reached [9].

On the other hand, membrane properties associated with the lipid composition affect not only PFTs binding but also other steps of pore-formation process [3d, 10]. The insertion of β-hairpins into more fluid membranes, such as 1,2-dioleoyl-*sn*-glycero-3-phosphocholine (DOPC)/cholesterol mixtures, is observed even before the full-circle LLO pore assembly is formed, resulting in smaller and less stable pores, which often open and close [5b]. Larger and less noisy LLO pores are formed with more ordered membranes of 1-palmitoyl-2-oleoyl-*sn*-glycero-3-phosphocholine (POPC)/cholest-erol mixtures [6b]. Smaller, structured aggregates of CDCs are called arcs and they represent not yet completed, but functional, circular assembly [11]. Arcs can also penetrate cholesterol-containing planar and supported lipid membranes and fuse with full-circle pores to form pores of irregular shape devoid of lipids in the lumen and which can be much larger than expected [6b, 12]. This is consistent with LLO biological function of penetrating the phagosomal membrane in order to promote

[a] Mirijam Kozorog, Gregor Anderluh*
Department for Molecular Biology and Nanobiotechnology
National Institute of Chemistry
Hajdrihova 19, 1000 Ljubljana, Slovenia
E-mail: gregor.anderluh@ki.si
[b] Marc-Antoine Sani, Frances Separovic*
School of Chemistry, Bio21 Institute
The University of Melbourne
VIC 3010, Australia
E-mail: fs@unimelb.edu.au

bacterial survival together with promoting other processes upon host infection [1c, 13].

In the present work, we observed the effect of LLO binding on cholesterol-rich lipid multilamellar vesicles (MLVs) using solid-state NMR. Differences were observed in the amount of bound protein and subsequently in the effect of LLO on MLVs of different composition of more fluid or more ordered lipid bilayers. Phospholipid acyl chain dynamics were significantly more perturbed for more fluid than more ordered bilayers, while membrane integrity was not affected, suggesting that LLO-membrane interactions do not cause loss of membrane structure. We also observed that cholesterol dynamics were affected upon toxin binding, with more effect observed in more fluid membranes.

Results and Discussion

Solid-state NMR was employed in order to describe the effects of LLO on lipid membranes of various compositions. ^{31}P and ^{2}H solid-state NMR, respectively, report on the phospholipid headgroups and deuterated acyl chains while ^{13}C T_1 and T_2 relaxation measurements were used to report on high and low frequency motions, respectively, of labelled cholesterol [14]. High cholesterol concentrations were used, since they are required for optimal interactions of LLO with lipid membranes [7a]. Membranes with different degree of saturation of acyl chains (POPC vs 1,2-dipalmitoyl-*sn*-glycero-3-phosphocholine (DPPC)) were included since membrane fluidity is proposed to affect the formation of CDC pores [10b] and also how cholesterol is presented to the CDC [8a]. The lipid fluidity for cholesterol-enriched POPC and DPPC and SM-containing bilayers have been reported previously [8a, 15]. In another case, POPC was partly substituted by 1-palmitoyl-2-oleoyl-*sn*-glycero-3-phosphoethanolamine (POPE), since smaller PE headgroup leads to more ordered membranes [16] and PE has been shown to reduce the cholesterol threshold for CDC binding to the target membrane [7c]. SM also has been shown to decrease the amount of accessible cholesterol and thus inhibit PFO association with cholesterol-rich membranes [8a]. Therefore, we also studied MLVs containing POPC, SM and cholesterol in order to observe the effects of LLO on domain-separated or raft-like membranes. ^{13}C-labeled cholesterol was used in order to detect the impact of bound LLO on cholesterol dynamics.

No significant changes were observed in ^{31}P and ^{2}H spectra of dPOPC/Chol (deuterated on POPC) membranes upon LLO binding at lipid:protein (L:P) ratio 500:1 (despite 97% bound LLO), indicating that there was insufficient amount of total protein bound to membranes to cause detectable changes in the lipid head groups (^{31}P NMR) or acyl chains (^{2}H NMR) of phospholipids (results not shown). On the other hand, at L:P ratio 125:1 both ^{31}P and ^{2}H NMR spectra showed an effect of LLO on PC/Chol bilayers.

LLO affects phospholipid headgroup mobility but does not disturb lipid bilayer organization.

^{31}P NMR experiments were run to investigate the effect of LLO on the lipid headgroup and membrane organization. LLO was incubated at 25°C with MLVs of various compositions. After centrifugation step, supernatants were removed along with unbound protein fractions. Bound LLO fractions varied from 85% to 92% in dPOPC or POPC/dPOPE bilayers containing 40 mol% of cholesterol but were heavily reduced in dPOPC/SM/Chol and dDPPC/Chol samples (Table 1). The results are in agreement with PFO results, where the presence of PE promoted while SM decreased the amount of bound protein [7c, 8a].

Table 1. The level of LLO binding to cholesterol-rich MLVs of various lipid compositions and effect of protein binding on ^{31}P chemical shift anisotropy and ^{2}H splittings of lipid chain CH_3 and plateau CH_2 groups[a].

Membrane lipid composition [b]	Lipid molar ratio (%)	Bound LLO	ΔΩ (%)[c]	Δν % (CH_3)[d]	Δν % (CH_2) (plateau)[d]
dPOPC/^{13}C-Chol	60:40	85%	-12.4	-14.2	-10.7
POPC/dPOPE/^{13}C-Chol	30:30:40	92%	-35.2	-19.2	-26.2
dPOPC/SM/^{13}C-Chol	30:30:40	40%	-2.7	-4.2	-1.9
dDPPC/^{13}C-Chol	60:40	21%	7.3	0	0.2

[a] The data were collected from one set of individual optimised experiments for each membrane type. [b] ^{13}C-Chol presents ^{13}C labelled cholesterol. [c] ΔΩ represents chemical shift anisotropy. [d] The difference in ^{2}H splittings. For [b-d] see also Figures 1 and 2.

The ^{31}P NMR spectra of LLO-bound MLVs were compared to those without the protein. All ^{31}P spectra showed typical bilayer powder patterns in the presence and absence of LLO, indicating that the bound protein did not disturb the lipid bilayer organization. However, the overall width of the spectra, which depends on the headgroup orientation and dynamics, varied between MLVs of different lipid compositions. In the case of cholesterol-rich MLVs of dPOPC/Chol and POPC/dPOPE/Chol a decrease in chemical shift anisotropy (CSA) was observed upon LLO binding, indicating increased headgroup mobility or disorder. The presence of SM or dDPPC lipids reduced this effect (Figure 1, Table 1), which would suggest that these more ordered bilayers impede insertion of LLO.

Hydrophobic core of more fluid membranes is perturbed upon LLO binding

The hydrophobic core perturbation was monitored by ^{2}H NMR using acyl chain deuterated phospholipids (Figure 2). Comparison of the effect of LLO protein on ^{13}C-Chol-enriched dPOPC or POPC/dPOPE bilayers showed a decrease in the quadrupolar splittings upon protein interactions; which indicates

that LLO significantly disordered the lipid bilayer core of dPOPC/Chol and POPC/dPOPE/Chol membranes, making it more fluid. This is consistent with a deeper insertion of LLO into more fluid lipid membranes. In the case of dDPPC/Chol or SM enriched membranes, LLO showed minor impact on the acyl chain order or dynamics, suggesting a superficial binding mode (Figure 2). ^{2}H NMR spectra support the ^{31}P NMR observation that LLO significantly disorders the more fluid PC/Chol but not the more ordered bilayers (including SM or DPPC).

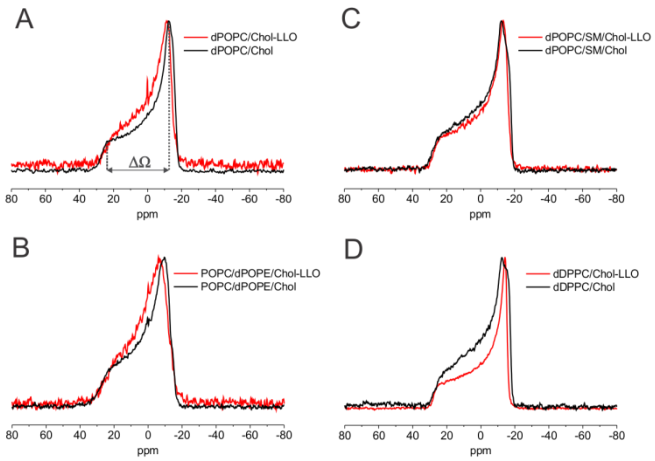

Figure 1. Static ^{31}P spectra of cholesterol-rich MLVs of various lipid compositions with and without bound LLO. MLVs were of: (A) dPOPC/^{13}C-Chol, (B) POPC/dPOPE/^{13}C-Chol, (C) dPOPC/SM/^{13}C-Chol, and (D) dDPPC/^{13}C-Chol. ΔΩ represents chemical shift anisotropy and Chol stands for ^{13}C labelled cholesterol.

LLO affects fast and slow motions of cholesterol

C3 and C4 ^{13}C labelled cholesterol was used in order to gain the insight into LLO-cholesterol interactions. The ^{13}C CPMAS spectrum of labelled cholesterol in dPOPC MLVs in the presence of LLO shows two high intensity signals from the C3 and C4 carbons of cholesterol (Figure 3). T_1 and T_2 ^{13}C relaxation measurements were performed to monitor LLO impact on the dynamics of cholesterol (Table 2). Using magic angle spinning (MAS) cross-polarization (CP) spin-inversion (T_1) and spin-echo (T_2) pulse sequences, the fast and slow motions of the cholesterol were shown to dramatically change in the presence of LLO for dPOPC/^{13}C-Chol and POPC/dPOPE/^{13}C-Chol membranes but not significantly in dDPPC/^{13}C-Chol or dPOPC/SM/^{13}C-Chol.

Interestingly, the molecular motions involving C4 are more disturbed than C3, which would suggest stronger interaction of the toxin with the C4 of cholesterol. Changes in T_1/T_2 ratio indicate an increase in low frequency motions of cholesterol [17]. The relative changes in T_1/T_2 ratios ^{13}C relaxation after LLO binding confirmed that the toxin interacts strongly with cholesterol in dPOPC (61 vs. 214) and POPC/dPOPE (69 vs. 161) but not in dPOPC/SM (70 vs. 91) or dDPPC (98 vs. 106) cholesterol-rich lipid systems (where the values in parentheses are T_1/T_2 ratio for C3 cholesterol in bilayers without vs. with LLO). This further supports a change in order for lipid/cholesterol due to binding of LLO as T_2 is influenced by motional averaging on a lower frequency timescale due to reorientation of the MLVs and/or translational diffusion over the membrane surface.

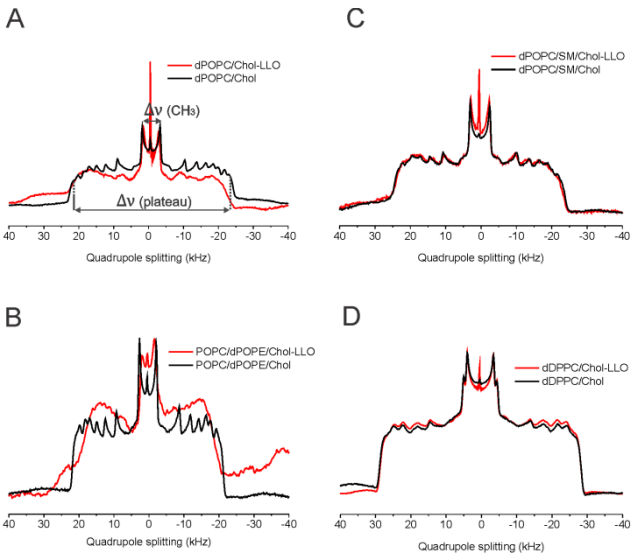

Figure 2. ^{2}H NMR spectra of cholesterol-rich MLVs of various lipid compositions with and without bound LLO. MLVs were of: (A) dPOPC/^{13}C-Chol, (B) POPC/dPOPE/^{13}C-Chol, (C) dPOPC/SM/^{13}C-Chol, and (D) dDPPC/^{13}C-Chol. Δν represents the differences in ^{2}H splittings of CH_3 and plateau CH_2 groups and Chol stands for ^{13}C labelled cholesterol.

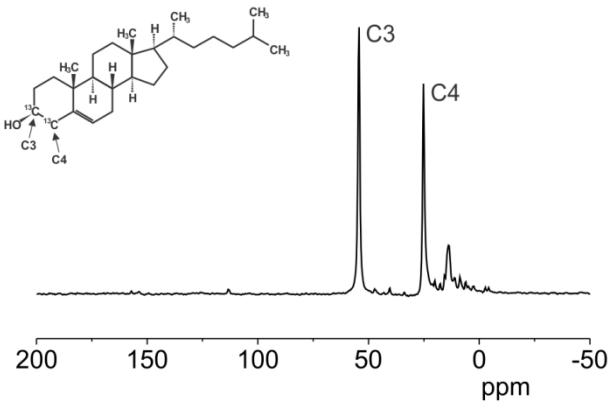

Figure 3. ^{13}C CPMAS spectra of dPOPC/^{13}C-Chol MLVs with bound LLO. Upper left inset: structural representation of cholesterol-3,4-^{13}C2. C3 and C4 indicate ^{13}C labelled cholesterol carbon peaks on ^{13}C CPMAS spectra and their position in cholesterol structure.

We have previously used surface plasmon resonance approach to study binding of LLO to liposomes composed of DOPC and

various sterols. We have shown that the binding was severely reduced in the case of cholesterol analogues with changes in the 3β-hydroxy group, such as cholesteryl acetate and 5-cholesten-3-one [7a]. The solid-state NMR data confirm this observation and indicate that there may exist a direct interaction of LLO with the C3 and C4 carbons of cholesterol.

Table 2. T_1 and T_2 relaxations of C3 and C4 cholesterol carbons of ^{13}C-Chol in the presence or absence of LLO at L:P ratio 125.

Lipid composition [a]	C3 T_1 (s)	C4 T_1 (s)	C3 T_2 (ms)	C4 T_2 (ms)
dPOPC/^{13}C-Chol	0.25±0.03	0.11±0.02	4.1±0.5	4.3±0.4
dPOPC/^{13}C-Chol+LLO	0.30±0.02	0.22±0.02	1.4±0.1	1.3±0.1
POPC/dPOPE/^{13}C-Chol	0.29±0.01	0.13±0.01	4.2±0.3	4.1±0.3
POPC/dPOPE/^{13}C-Chol+LLO	0.29±0.02	0.35±0.03	1.8±0.1	1.7±0.1
dDPPC/^{13}C-Chol	0.39±0.01	0.20±0.01	4.0±0.3	3.7±0.2
dDPPC/^{13}C-Chol+LLO	0.37±0.01	0.20±0.01	3.5±0.2	2.9±0.1
dPOPC/SM/^{13}C-Chol	0.32±0.01	0.17±0.01	4.6±0.4	4.0±0.3
dPOPC/SM/^{13}C-Chol+LLO	0.30±0.01	0.19±0.01	3.3±0.1	3.0±0.1

[a] ^{13}C-Chol presents ^{13}C labelled cholesterol.

Chemical shift changes of ^{19}F-LLO labelled on tryptophans upon membrane binding

Since significant differences in the membrane lipid dynamics and in the level of LLO binding to cholesterol-rich membranes of different lipid compositions were observed (Tables 1-2, Figures 1-3), we checked if the lipid composition affected LLO binding to the membrane. Therefore, the ^{19}F spectra of LLO with all seven tryptophan residues labelled with ^{19}F were recorded upon binding to different membranes. Since 6 out of 7 tryptophans are in the membrane binding domain of LLO (structural Domain 4), insight into protein binding could be gained by such approach [18]. The ^{19}F spectra of LLO tryptophans showed differences in chemical shifts upon binding to the cholesterol-rich MLVs with different degrees of fluidity (Figure 4).

The NMR spectra of LLO bound to dPOPC/Chol and POPC/dPOPE/Chol membranes show high similarity with three separate clusters of peaks (Figure 4), which suggests that the tryptophans are in a similar chemical environment in both types of membranes. The peak positions are distinct from those of the spectra of the unbound protein in buffer. The most change was observed at around -124.5 ppm and -119.9 ppm, where bound LLO lacks the spectral intensity seen in the free protein in buffer (see the dotted lines in Figure 4). As we have previously shown [18a], the peaks at around -124.5 ppm were assigned to W489, W491 and W189 in unbound protein and two of them (W489 and W189) experienced a change in chemical shift upon binding to POPC/Chol MLVs. W489 and W491 lie exposed at the bottom of Domain 4 [4a] and probably insert into the membrane upon binding. W189 lies in Domain 1 and has been proposed to be involved in subsequent stages of pore formation, as was supported by mutations and activity studies [18a]. Additional density at -118.5 ppm in the membrane-bound LLO is due to W189 chemical shift change. Higher intensity for that peak arises from W512, which shifts to the same position from -120 ppm where the peak is found for free protein in buffer.

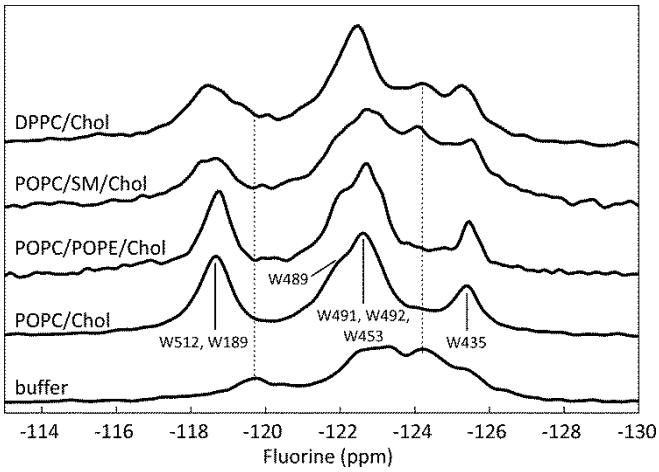

Figure 4. MAS solid-state NMR spectra of ^{19}F labelled LLO, bound to different cholesterol-rich lipid membranes compared to non-spinning NMR spectra of unbound protein in buffer. LLO tryptophan contribution was previously assigned to different peaks [18] and is indicated here for the POPC/Chol membranes.

By contrast, in the presence of more ordered MLVs with DPPC or SM, i.e., dDPPC/Chol and dPOPC/SM/Chol MLVs, not all ^{19}F-labelled LLO tryptophan resonances shifted in a similar manner as for POPC or POPE membranes (Figure 4), despite having the same cholesterol molar ratio. The signal intensity at -120 ppm seen in unbound LLO spectra arising from W512, however, decreased also in the bound LLO spectra for the more ordered membranes. There were also no changes in chemical shift of W435 (-125.5 ppm) or W491, W492 and W453 (around -122 ppm). Similarly, all bound LLO spectra exhibit additional density at the position of bound W189 and W512 (-118.5 ppm) but it is less intense in the case of dDPPC/Chol and dPOPC/SM/Chol membranes, suggesting that tryptophan residues are not in a similar chemical environment as when bound to POPC or POPE membranes. However, the biggest differences in the ^{19}F spectra of DPPC or SM containing membranes are due to the presence of the signal intensity at around -124 ppm, which is the position of the chemical shift of W189 in the unbound LLO protein and proposed to be involved in oligomerization, an inevitable step in pore-formation process. The changes in ^{19}F NMR spectra may thus reflect an inability of LLO to fully insert into these membranes or suggest different mechanism for LLO interactions with membrane systems with different fluidity, e.g. oligomeric assemblies of LLO that interact differently with membranes. The ^{19}F-NMR results are also in agreement with the observed

differences in ^{2}H and ^{31}P spectra and T_1/T_2 relaxation times differences of ^{13}C-cholesterol in different membranes upon LLO binding.

Conclusions

Solid-state NMR experiments showed that cholesterol availability and the fluidity of the lipid membrane systems are critical to achieve high membrane binding and conformational homogeneity of LLO, a CDC with interesting and unique features. ^{31}P and ^{2}H NMR experiments with cholesterol-rich deuterated phospholipid MLVs showed a significant effect of LLO on the acyl chain dynamics and similar effect on the phospholipid headgroups for POPC/Chol and POPC/POPE/Chol bilayers (Table 1), while DPPC/Chol and POPC/SM/Chol bilayers, despite lower amount of bound protein, were hardly affected. Furthermore, ^{13}C relaxation studies of phospholipid bilayers with two ^{13}C labelled cholesterol carbons (C3, C4) showed a more dramatic effect in the more fluid POPC/Chol and POPC/POPE/Chol bilayers upon incubation with LLO whereas the change was not significant for the more ordered bilayers. The results, therefore, are in agreement with deeper insertion of LLO into more fluid (or liquid disordered) cholesterol-rich phospholipid bilayers, which probably further relate to pore assembly. We also demonstrate changes in cholesterol dynamics, which indicate cholesterol interactions with LLO upon binding.

Experimental Section

Materials

1-palmitoyl-2-oleoyl-*sn*-glycero-3-phosphocholine (POPC), 1-palmitoyl-d31-2-oleoyl-*sn*-glycero-3-phosphocholine (dPOPC), 1,2-dipalmitoyl-d31-*sn*-glycero-3-phosphocholine (dDPPC), 1-palmitoyl-d31-2-oleoyl-*sn*-glycero-3-phosphoethanolamine (dPOPE) and sphingomyelin (SM) were from Avanti Polar Lipids. Cholesterol-3,4-$^{13}C2$ (^{13}C-chol) was from Cambridge Isotope Laboratory. All other chemicals were from Sigma, unless stated otherwise.

LLO preparation

Recombinant LLO with histidine tag, TEV protease cleavage site and all seven tryptophans isotopically labelled with ^{19}F was expressed in *E. coli* BL21(DE3) trp::Tn10 strain by adding 5F-Trp into M9 minimal medium, as described recently in detail [18a]. After overnight growth at 20°C the cells were harvested by centrifugation and lysed by sonication. The protein was purified from filtered supernatant on IMAC Sepharose HP column (GE Healthcare) as described [6b]. Eluted hexa-histidine-tagged LLO was dialyzed overnight in the presence of TEV protease, which was removed next day together with the histidine-tag by another IMAC step. The protein was concentrated and exchanged with final morpholineethanesulfonic (MES) buffer (20 mM MES, pH 5.7, 150 mM NaCl, 5% glycerol, 2 mM dithiothreitol). This procedure routinely yielded around 10-16 milligrams of pure homogeneous recombinant LLO per 1 l culture.

Solid-state NMR sample preparation – MLVs with and without bound LLO

Different lipid mixtures all with 40 mol % cholesterol were prepared with and without LLO. Firstly, lipids were co-dissolved with cholesterol in chloroform/methanol mixture (3:1 vol:vol) in a round bottom flask. The solvent was removed by rotary evaporation and lipid films were afterwards hydrated in Milli-Q water and lyophilised over-night, as described in Weber et al. [19]. LLO in final MES buffer at pH 5.7 was added to the dry lipid powders of desired composition with lipid/protein ratio 125:1. The mixtures were incubated for 30 min at 25°C and freeze-thawed (-196°C/25°C) three times afterwards, followed by centrifugation for 10 min at top speed in benchtop centrifuge at 20°C. Pellet was weighed, frozen and packed into a 4 mm NMR rotor by centrifugation technique, while the absorbance at 280 nm in the supernatant was measured to check the unbound protein concentration. Lipid samples without the protein were hydrated in MES buffer without the presence of LLO and in all other aspects prepared in the same way. Unbound LLO in buffer at 0.3 mM concentration was pipetted directly into the rotor.

While optimizing NMR experiments LLO was incubated with dPOPC/(^{13}C-)Chol membranes several times at different lipid:protein ratios. The bound fraction was repeatedly high (83 ± 13 %) at final 125:1 lipid:LLO ratio. The data in Table 1 are from the optimized experiments from the final NMR samples prepared with different membrane compositions.

NMR experiments

The solid-state NMR experiments were conducted on a Bruker 400 MHz NMR equipped with HFXY 4 mm MAS probe with the bearing air supply of the NMR probe set to 25°C. All spectra were processed using NMRPipe.

Static phosphorus NMR spectra were obtained at 161.98 MHz using a Hahn echo pulse sequence with proton decoupling. Typically a 6 µs 90° pulse was used with 40 µs echo time and 3 s recycle delay. 16 k scans were collected and processed with 100 Hz exponential line-broadening. ^{31}P spectra were externally referenced to 0 ppm using H_3PO_4 prior to each experiment. The ΔΩ value (^{31}P chemical shift anisotropy) was calculated by using Equation 1:

$$\Delta\Omega\ (\%) = \frac{\Delta\Omega\ (lipids\ with\ LLO) - \Delta\Omega\ (lipids)}{\Delta\Omega\ (lipids)} \times 100 \qquad \text{Equation 1}$$

where ΔΩ is the static ^{31}P chemical shift anisotropy of lipids in the presence or absence of LLO.

Static deuterium experiments were performed at 61.42 MHz using a solid-echo sequence with high power decoupling. A 8.5 µs 90° pulse was used with 40 µs echo delay, and 0.5 s recycle time. Although the pulse length was not optimal (30 kHz excitation) and the deuterium spectra showed some power roll off, the quality was sufficient to compare effect of LLO on phospholipid membranes. A minimum of 65k scans were collected and Fourier transformed. The value (%) of differences in ^{2}H splittings of lipid CH_3 and plateau CH_2 groups upon LLO binding were calculated using Equation 2:

$$\Delta\nu\ (\%) = \frac{\Delta\nu\ Value\ (lipids\ with\ LLO) - \Delta\nu\ Value\ (lipids)}{\Delta\nu\ Value\ (lipids)} \times 100 \qquad \text{Equation 2}$$

where Δν Value is the difference in ^{2}H splittings of lipids in the presence or absence of LLO.

^{13}C cross-polarization (CP) magic angle spinning (MAS) experiments were carried out using a ^{1}H excitation pulse of 80 kHz, followed by a CP contact time of 1.5 ms using 46 kHz field on ^{13}C and a ^{1}H SPINAL64 decoupling at 80 kHz during acquisition, a spinning rate of 10 kHz, and a recycle delay of 4 s. The FIDs were zero-filled to 16k points and 100 Hz line broadening was applied.

T_1 and T_2 relaxations experiments were performed using CPMAS with a 10 kHz spinning rate. Laboratory frame spin-lattice (T_1) and spin-spin (T_2) relaxation times were measured by the inversion-recovery and spin-echo method, respectively [17]. Typically a 5.4 µs ^{13}C 90° pulse and 4 s recycle delay were used. 512 scans were collected and processed. The ratio of T_1 and T_2 values of C3 and C4 cholesterol carbons in the presence of LLO, compared to MLVs without the protein were calculated.

^{19}F MAS experiments were performed at 376.5 MHz. Other parameters were ~ 56 kHz single pulse excitation with ~ 55 kHz SPINAL64 ^{1}H decoupling, a 5 s recycle delay, a spectral width of 250 kHz, 8 k complex points acquisition zero-filled to 32k points and 75 Hz line broadening. Prior to each MAS experiment ^{19}F spectra were externally referenced using trifluoroacetic acid (-76.5 ppm). Between 16k and 48k scans were acquired for the static and MAS ^{19}F NMR spectra.

Acknowledgements

MK and GA acknowledge the support of the Slovenian Research Agency (Program grant Molecular interactions P1-0391), EN-FIST Centre of Excellence, and Slovene Human Resources Development and Scholarship Fund. M-AS and FS acknowledge Australian Research Council LIEF support for solid-state NMR.

Keywords: Listeriolysin O • Cholesterol dependent cytolysins • Solid state NMR • Lipid membranes • Pore forming toxins

[1] a) D. A. Portnoy, P. S. Jacks and D. J. Hinrichs, *J. Exp. Med.* **1988**, *167*, 1459-1471; b) P. Cossart, M. F. Vicente, J. Mengaud, F. Baquero, J. C. Perez-Diaz and P. Berche, *Infect. Immun.* **1989**, *57*, 3629-3636; c) M. A. Hamon, D. Ribet, F. Stavru and P. Cossart, *Trends Microbiol.* **2012**, *20*, 360-368.

[2] a) K. E. Beauregard, K. D. Lee, R. J. Collier and J. A. Swanson, *J. Exp. Med.* **1997**, *186*, 1159-1163; b) M. M. Gedde, D. E. Higgins, L. G. Tilney and D. A. Portnoy, *Infect. Immun.* **2000**, *68*, 999-1003; c) C. L. Birmingham, V. Canadien, N. A. Kaniuk, B. E. Steinberg, D. E. Higgins and J. H. Brumell, *Nature* **2008**, *451*, 350-354.

[3] a) R. J. Gilbert, *Structure* **2005**, *13*, 1097-1106; b) E. M. Hotze and R. K. Tweten, *Biochim. Biophys. Acta* **2012**, *1818*, 1028-1038; c) E. M. Hotze, H. M. Le, J. R. Sieber, C. Bruxvoort, M. J. McInerney and R. K. Tweten, *Infect. Immun.* **2013**, *81*, 216-225; d) M. Marchioretto, M. Podobnik, M. Dalla Serra and G. Anderluh, *Biophys. Chem.* **2013**, *182*, 64-70.

[4] a) S. Koster, K. van Pee, M. Hudel, M. Leustik, D. Rhinow, W. Kuhlbrandt, T. Chakraborty and O. Yildiz, *Nat. Commun.* **2014**, *5*, 3690; b) J. Rossjohn, S. C. Feil, W. J. McKinstry, R. K. Tweten and M. W. Parker, *Cell* **1997**, *89*, 685-692.

[5] a) D. W. Schuerch, E. M. Wilson-Kubalek and R. K. Tweten, *Proc. Natl. Acad. Sci. U.S.A.* **2005**, *102*, 12537-12542; b) A. Bavdek, R. Kostanjsek, V. Antonini, J. H. Lakey, M. Dalla Serra, R. J. Gilbert and G. Anderluh, *FEBS J.* **2012**, *279*, 126-141.

[6] a) R. K. Tweten, E. M. Hotze and K. R. Wade, *Ann. Rev. Microbiol.* **2015**, *69*, 323-340; b) M. Podobnik, M. Marchioretto, M. Zanetti, A. Bavdek, M. Kisovec, M. M. Cajnko, L. Lunelli, M. Dalla Serra and G. Anderluh, *Sci. Rep.* **2015**, *5*, 9623; c) G. Anderluh and J. H. Lakey, *Trends Biochem. Sci.* **2008**, *33*, 482-490.

[7] a) A. Bavdek, N. O. Gekara, D. Priselac, I. Gutierrez Aguirre, A. Darji, T. Chakraborty, P. Maček, J. H. Lakey, S. Weiss and G. Anderluh, *Biochemistry* **2007**, *46*, 4425-4437; b) A. P. Heuck, E. M. Hotze, R. K. Tweten and A. E. Johnson, *Mol. Cell* **2000**, *6*, 1233-1242; c) Y. Ohno-Iwashita, M. Iwamoto, S. Ando and S. Iwashita, *Biochim. Biophys. Acta* **1992**, *1109*, 81-90; d) E. Rosenqvist, T. E. Michaelsen and A. I. Vistnes, *Biochim. Biophys. Acta* **1980**, *600*, 91-102; e) C. R. Alving, W. H. Habig, K. A. Urban and M. C. Hardegree, *Biochim. Biophys. Acta* **1979**, *551*, 224-228.

[8] a) J. J. Flanagan, R. K. Tweten, A. E. Johnson and A. P. Heuck, *Biochemistry* **2009**, *48*, 3977-3987; b) L. D. Nelson, A. E. Johnson and E. London, *J. Biol. Chem.* **2008**, *283*, 4632-4642.

[9] B. B. Johnson and A. P. Heuck in *MACPF/CDC Proteins- Agents of Defence, Attack and Invasion* (Eds.: G. Anderluh and R. Gilbert), Springer Netherlands, **2014**, pp. 63-81.

[10] a) T. Praper, A. Sonnen, G. Viero, A. Kladnik, C. J. Froelich, G. Anderluh, M. Dalla Serra and R. J. Gilbert, *J. Biol. Chem.* **2011**, *286*, 2946-2955; b) N. Rojko and G. Anderluh, *Accounts Chem. Res.* **2015**, 48, 3073-3079.

[11] a) R. J. Gilbert, M. Dalla Serra, C. J. Froelich, M. I. Wallace and G. Anderluh, *Trends Biochem. Sci.* **2014**, *39*, 510-516; b) R. J. Gilbert, M. Mikelj, M. Dalla Serra, C. J. Froelich and G. Anderluh, *Cell. Mol. Life Sci.* **2013**, *70*, 2083-2098.

[12] a) Y. Ruan, S. Rezelj, A. Bedina Zavec, G. Anderluh and S. Scheuring, *PLoS Pathog.* **2016**, *12*, e1005597; b) E. Mulvihill, K. van Pee, S. A. Mari, D. J. Muller and O. Yildiz, *Nano Lett.* **2015**, *15*, 6965-6973.

[13] L. M. Shaughnessy, A. D. Hoppe, K. A. Christensen and J. A. Swanson, *Cell. Microbiol.* **2006**, *8*, 781-792.

[14] A. Drechsler and F. Separovic, *IUBMB Life* **2003**, *55*, 515-523.

[15] a) R. F. de Almeida, A. Fedorov and M. Prieto, *Biophys. J.* **2003**, *85*, 2406-2416; b) M. B. Lande, J. M. Donovan and M. L. Zeidel, *J. Gen. Physiol.* **1995**, *106*, 67-84.

[16] F. Separovic and K. Gawrisch, *Biophys. J.* **1996**, *71*, 274-282.

[17] B. A. Cornell, J. B. Davenport and F. Separovic, *Biochim. Biophys. Acta* **1982**, *689*, 337-345.

[18] a) M. Kozorog, M. A. Sani, M. Lenarčič Živkovič, G. Ilc, V. Hodnik, F. Separovic, J. Plavec and G. Anderluh, *Sci. Rep.* **2018**, *8*, 6894; b) S. L. Grage, J. Wang, T. A. Cross and A. S. Ulrich, *Biophys. J.* **2002**, *83*, 3336-3350.

[19] D. K. Weber, M. A. Sani, M. T. Downton, F. Separovic, F. R. Keene and J. G. Collins, *J. Am. Chem. Soc.* **2016**, *138*, 15267-15277.

FULL PAPER

Listeriolysin O is a cholesterol-dependent cytolysin, responsible for the escape of pathogenic bacteria, *Listeria monocytogenes*, from the acidic phagolysosome. Listeriolysin O binds cholesterol-rich membranes, oligomerizes and forms pores by inserting parts of its polypeptide chain into the membrane. Solid-state NMR experiments showed that listeriolysin O preferentially binds and perturbs the hydrophobic core of more fluid cholesterol-rich membranes.

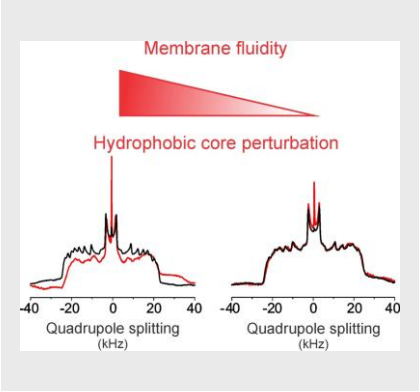

Mirijam Kozorog, Marc-Antoine Sani, Frances Separovic and Gregor Anderluh**

Page No. – Page No.

Listeriolysin O binding affects cholesterol and phospholipid acyl chain dynamics in fluid cholesterol-rich bilayers